

# Dynamic Loading of LIGA Structures

Wei-Yang Lu, Helena Jin, Simon Lee  
Sandia National Laboratories, P.O. Box 969, MS9409, Livermore, CA 94551-0969

Kenneth Gwinn  
Sandia National Laboratories, MS0372, Albuquerque, NM 87123

Weinong Chen, Bo Song  
School of Aeronautics and Astronautics, and School of Materials Engineering  
Purdue University, West Lafayette, IN 47907-2023

## ABSTRACT

Microsystem components must survive a certain range of shock and vibration environments in many applications. It is essential that the performance of these new microsystem components is well characterized and understood under such dynamic loading. This paper presents a study of LIGA structures subject to high strain rate loading. A Hopkinson bar setup was utilized to provide the shock environment for these devices. By varying the striker size, the pulse shaper size, and the striker velocity (or the pressure of the compressed air), desired loading profiles were generated at the free end of the input bar, where the fixture and specimen were attached. During the experiment, the deformation and displacement of the specimen were recorded by a high speed digital camera. Finite element simulations of the experiments by considering large elastic deformations were also obtained based on the experimentally measured velocity profile as the loading input. Experimental and simulated results are compared and discussed.

## INTRODUCTION

Microsystems fabricated from SMM and LIGA processes have gradually integrated into engineering applications. Similar to all other engineering component, it is important to understand and evaluate the static and dynamic properties of these new micro-devices and materials before they are deployed in applications. Especially in some critical cases, the system may be subjected to severe shock and vibration environments. The reliability and survivability of the systems needs to be assessed.

Modeling and simulation have been successful in predicting the performance of many engineering systems, but models for Microsystems under high strain rate of loading have not been validated. Comparing SMM or LIGA Microsystems with conventional engineering components, they differ both in size and materials. The size difference is apparent. As for materials, polysilicon becomes the structural material of SMM Microsystems, and the LIGA process has a wide selection of materials, including metal alloys, polymers, and ceramics. It is known that the mechanical properties of the materials of the Microsystems are largely influenced by the fabrication parameters and may be different from those in the bulk form. The experiments and data of strain-rate dependent mechanical behaviors are currently needed for model calibration and validation as well as performance evaluation of Microsystems in dynamic environments.

In the present work, experiments are developed to investigate the deformation of LIGA cantilever specimens under impact loading conditions. Cantilever is an elementary structural component and is commonly used in Microsystems. Experimental results are compared with model simulations.

## EXPERIMENTAL SETUP AND CALIBRATION

The experimental setup is based on a modified Hopkinson Bar apparatus with pulse shaping techniques, which enables us to generate desired shock environments for micro specimens at the free end of the incident bar, for example, a short pulse of near constant acceleration and deceleration. Since the characteristics of a shock wave are influenced by the speed and size of the striker and the geometry and material of the pulse shaper, it is necessary to calibrate the particle speed (or the impulse function) at the free end of a Hopkinson bar with various pulse shapers and strikers before impact experiments.



Figure 1 Schematic diagram of Hopkinson Bar set up for impact experiment.

A schematic diagram of the Hopkinson bar impact setup is shown in Figure 1. The transmission bar was not needed in the experiment, therefore, not included. A fixture for micro specimens (or Microsystems) was placed at the end of the incident bar. The fixture could be either a separate component that was just in contact with the bar or an integral part that was firmly attached to the bar. During the calibrating process, the speed of the fixture  $v$  was determined by two methods: one was directly measured from a laser vibrometer, and the other was calculated from the strain  $\varepsilon$ , measured by the strain gage, and the equation  $v = 2c\varepsilon$ , where  $c$  is the wave speed of the bar. The purpose of the laser vibrometer measurement was to verify the strain gage result and was used only during the calibration process.

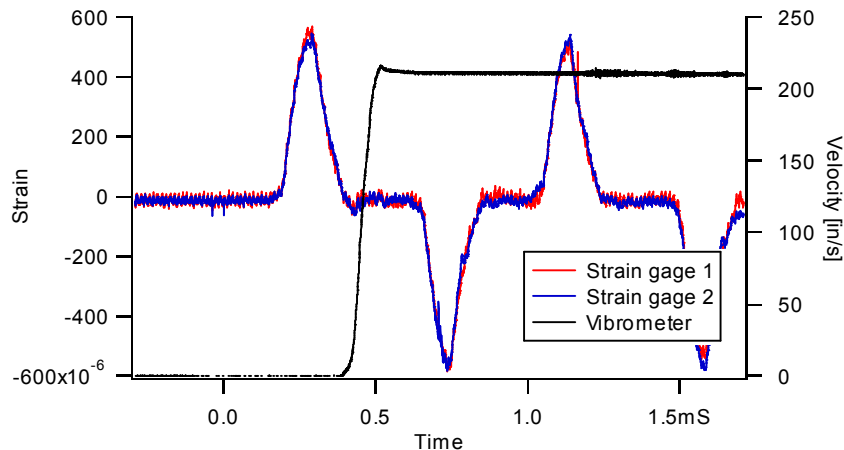


Figure 2 Strain and velocity signals from strain gages and vibrometer.

Figure 2 displays a typical strain and velocity history of an impact experiment, where the micro specimen fixture was a separate component just in contact with the incident bar. After the striker impacted the bar, the stress wave propagated toward the free end and then reflected back. It traveled back and forth as indicated by the strain gage signal. The laser vibrometer signal showed a time delay since it measured the particle velocity of the fixture at the free end, not at the strain gage. The amount of time delay is equal to half of the period between the incident and reflected waves on the strain gage signal. With a proper time shift, the strain gage and vibrometer results are plotted in Figure 3(a). The speed of the free end, calculated from the strain gage data, changed from zero to 210 in/s and returned to zero. The speed of the fixture, measured directly from the vibrometer, was

consistent with the speed of the free end during the acceleration period, but the fixture started to fly away at a constant speed as soon as it reached the maximum speed. Figure 3(b) shows another example, where the fixture is tightly connected to the incident bar and there is a period of constant speed in the loading profile. Both cases show that the velocity-time curve obtained from the strain gage data correctly represents the speed of the fixture at the end of the bar.

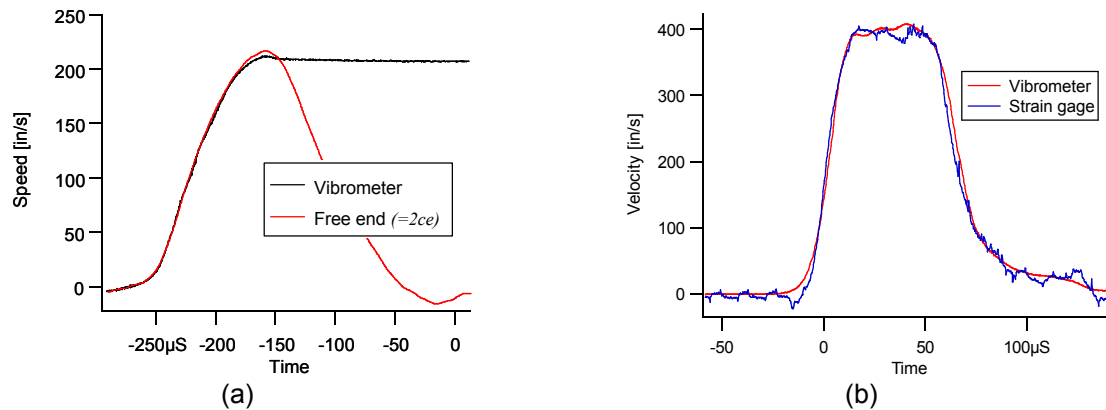


Figure 3 Velocities of the fixture of two different setups and loading profiles: (a) The fixture is a separate element and placed in contact with the free end of the Hopkinson bar, (b) the fixture is firmly attached to the bar.

## IMPACT EXPERIMENTS OF MICRO SPECIMENS

The specimens involved in the impact experiments were tapered beam-mass structure manufactured from LIGA micro-fabrication process. The drawing of the specimen design is shown in Figure 4. The structure was made of Ni, electrodeposited using Watts bath with saccharin. (Saccharin is included as a stress reliever and results in a very fine grain size on the order of 10 – 20 nm.) A typical quasi-static tensile stress-strain curve of such Watts bath-deposited Ni is shown in Figure 5. The yield and ultimate tensile stresses are approximately  $\sigma_y = 1,200$  and  $\sigma_{ut} = 1800$  MPa, respectively. From a number of characterization experiments, LIGA Ni data also display a correlation between the yield stress and Vickers micro-hardness (using 25 g load) following the relation:

$$\sigma_y = -300 + 3 H_{25g}$$

where  $\sigma_y$  is in MPa. The equation allows us to use hardness measurement as a surrogate for yield stress [1]. Accurate characterization of the elastic modulus of LIGA-fabricated specimens has been difficult due to the small size and alignment considerations. For regular Watts bath-deposited Ni, the elastic modulus falls in the range:  $165 < E < 190$  GPa [2]. The mechanical properties of the LIGA deposited material are known to be influenced by the feature size of the structure and the fabrication process. A direct measurement of the properties of this batch of specimens was not performed; however, the Vickers microhardness of the specimens were measured  $H_{25g} = 530$ . The hardness value gives an estimated yield stress of 1,290 MPa.

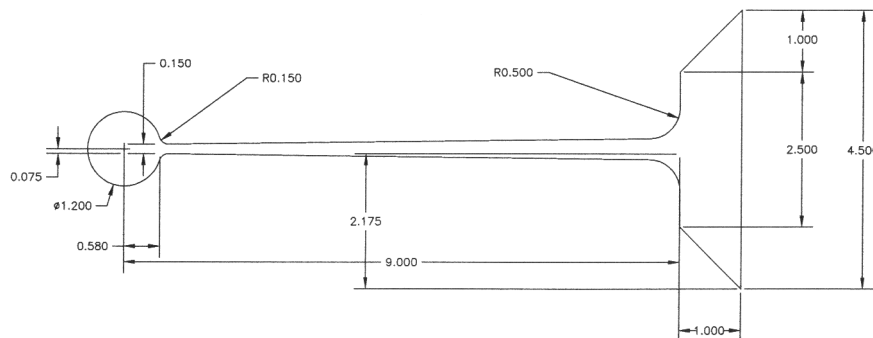


Figure 4 LIGA Ni tapered beam–mass structure, dimensions in mm.

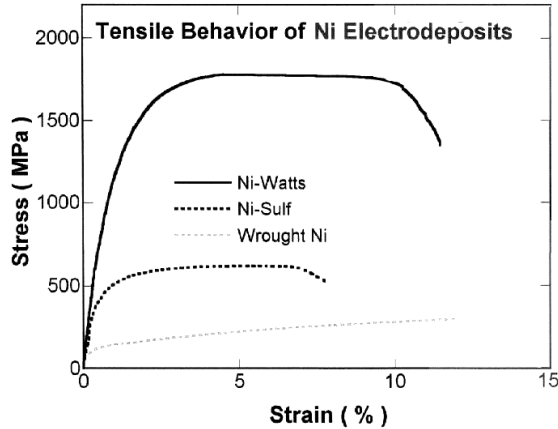


Figure 5 Stress-strain behavior of electrodeposited and wrought Ni. Using Watts bath with saccharin results in a fine grain size Ni deposit with high-strength. (Reproduced from Kelly and Goods [1])

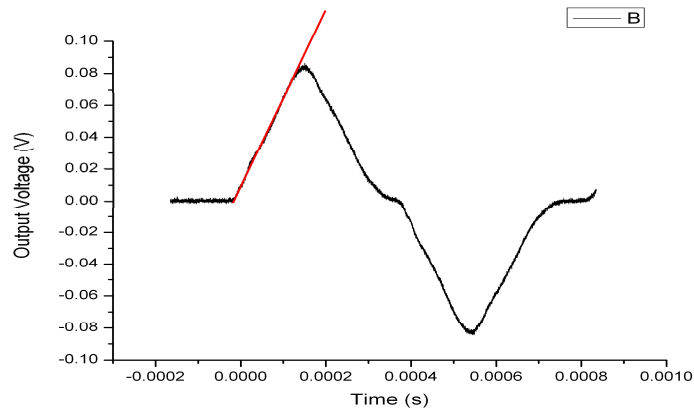


Figure 6 Original oscilloscope record of 20k g impact.

In a typical 20k g impact experiment, the pulse profile is shown in Figure 6, which is the original oscilloscope record of the strain gage data. The time that the free end of the bar starts to move is defined as  $t = 0$ . A linear fit of the curve between 0 and 160  $\mu$ s indicated a constant acceleration  $a \approx 20,000$  g; similarly, a constant deceleration  $a \approx -20,000$  g was between 160 and 360  $\mu$ s. (The exact number calculated is  $a = 19,749$  g.) The positive output voltage was proportional to the particle velocity at the free end of the incident bar. The voltage was zero at time  $t = 320$   $\mu$ s, so was the velocity of the free end. Negative output voltage, however, did not represent the speed at the free end since it meant the reflected tensile wave traveled towards the impact end and the free end remained still.

Sequential images of the deformed tapered beam-mass structure under 20k g impact are shown in Figure 7. A high-speed digital camera (Cordin 550), triggered by the strain gage signal, was utilized to capture the deformation of the micro specimen. The first 550  $\mu$ s of the experiment was recorded, which was slightly longer than the shock loading duration 360  $\mu$ s. The high-speed digital camera was set at the speed of 51,037 frames per second (fps), corresponding to a sampling period of 19.6 microseconds. The figure displays every fourth of the frames recorded. In Figure 7(f), (g) and (h), the bar stayed at the same location indicating that the end of the bar had stopped moving. The displacements of the bar and the mass ( $u_{bar}$  and  $u_{mass}$ ) can be measured from the images as shown in Figure 8, where Frame #14 ( $t = 196$   $\mu$ s) lies on top of Frame #04 ( $t = 0$   $\mu$ s). The measured values are  $u_{bar} = 3.645$  mm and  $u_{mass} = 1.024$  mm. Frame #14 shows the minimum relative displacement  $u_{rel} = u_{mass} - u_{bar} = -2.621$  mm observed from the captured images. The actual minimum value of  $u_{rel}$  may be somewhat smaller and occurred at a slightly different time.

Although the deformation and oscillation of the tapered cantilever-mass structure is not available for  $t > 550 \mu\text{s}$  due to the limitation of the recording device, the post-experiment specimen provide some interesting information. The structure appears to be in the same form as pre-experiment, i.e., there is no apparent plastic deformation, crack, or damage.

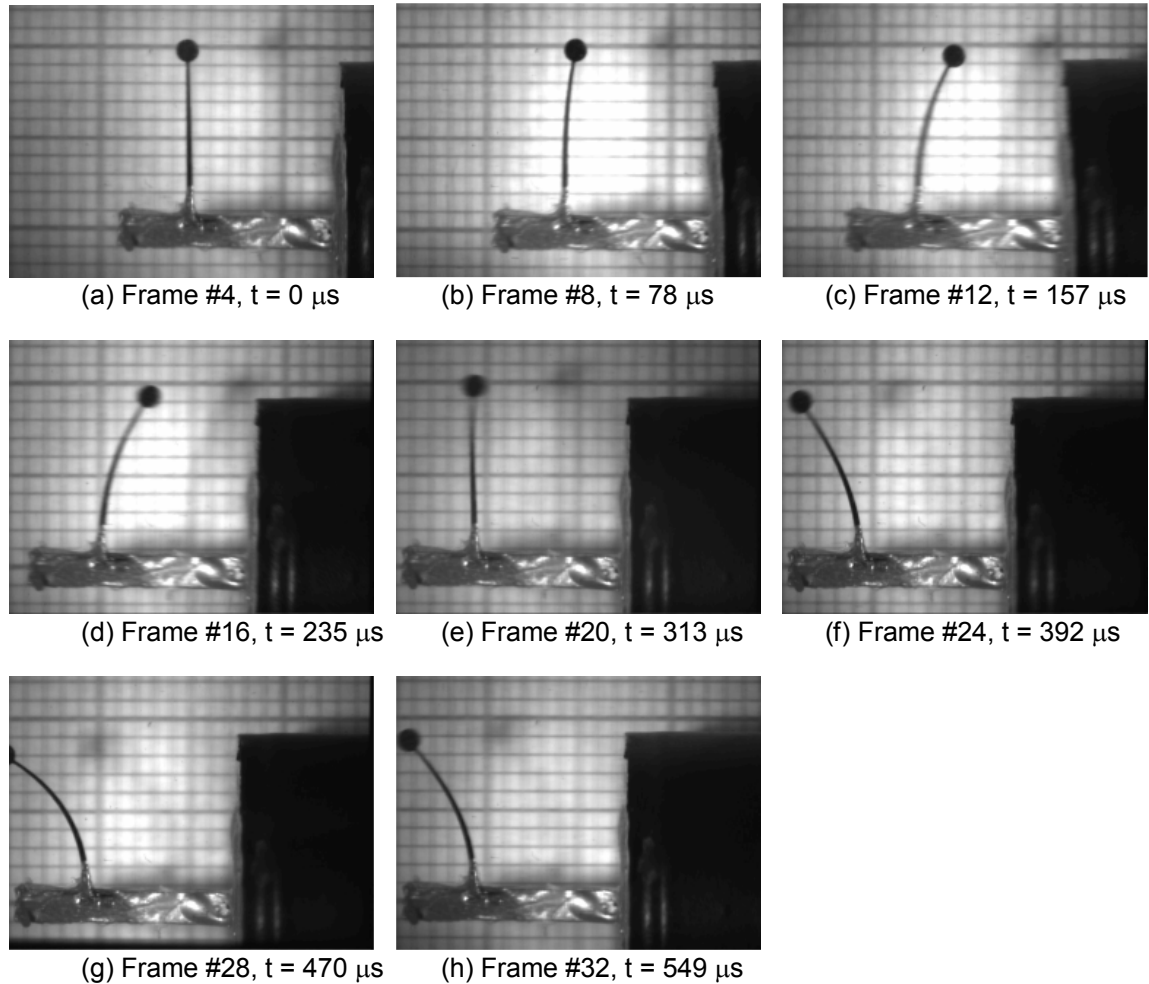


Figure 7 Images of the deformed tapered beam-mass structure under the 20k g impact.

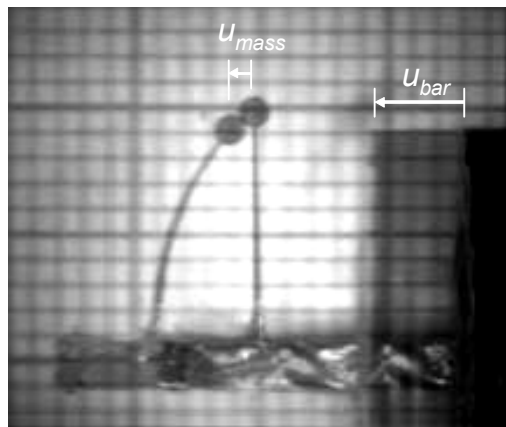


Figure 8 Displacements  $u_{\text{mass}}$  and  $u_{\text{bar}}$  at  $t = 196 \mu\text{s}$  are measured from Frame #4 & 14.

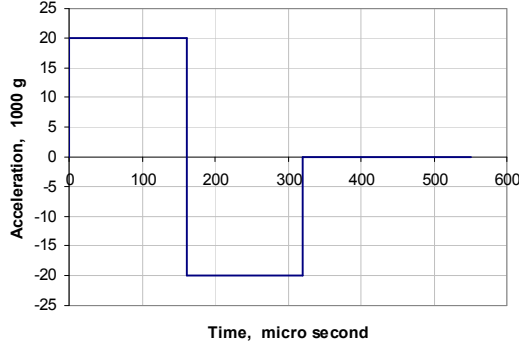


Figure 9 Idealized shock profile for model simulation.

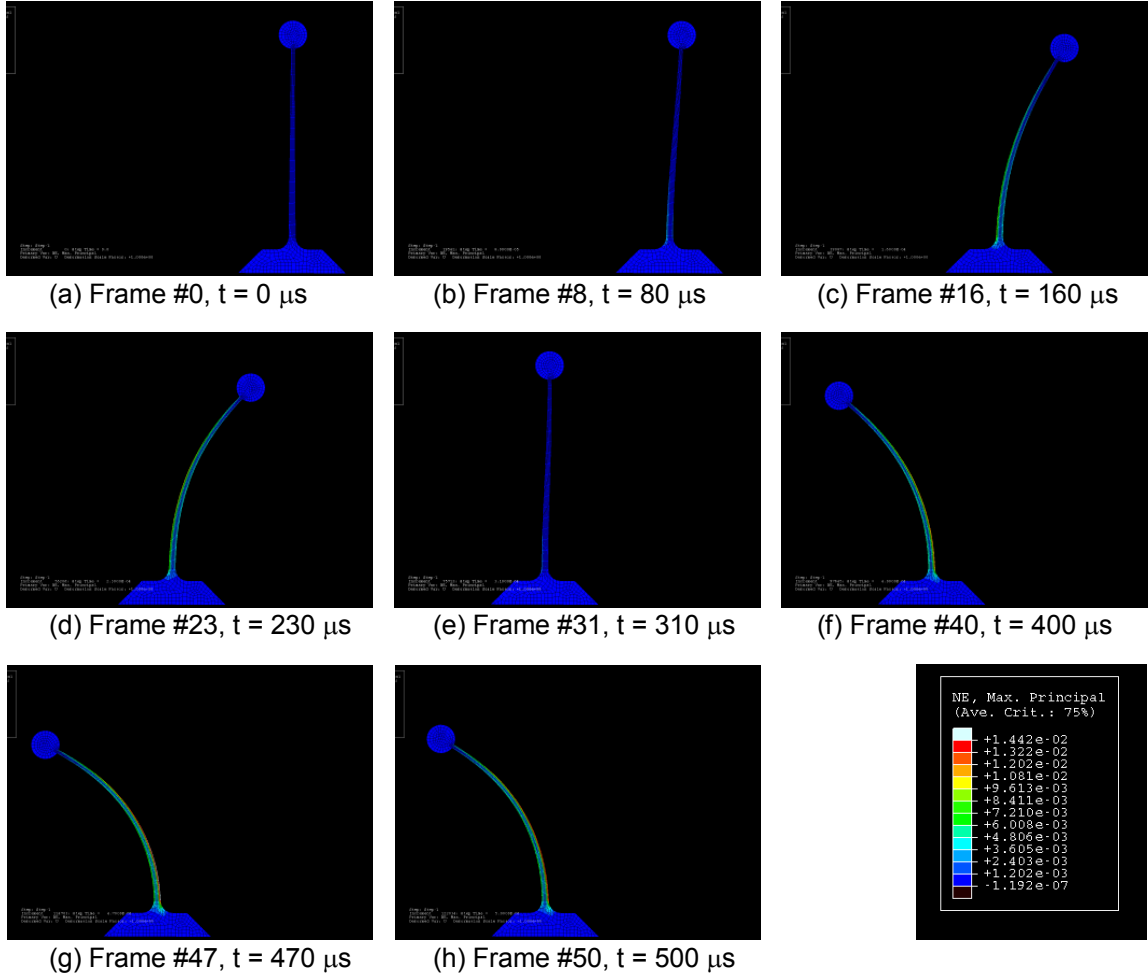


Figure 10 Results of simulation of the impact experiment.

Numerical simulation of the shock experiment was conducted by using ABACUS/explicit elastic model. The model assumes linear material properties and nonlinear deformation (i.e. large deformation and rotation are allowed). The following material properties of LIGA Ni were selected: Young's modulus  $E = 200$  GPa, Poisson ratio  $\nu = 0.3$ , and density  $\rho = 8,800$  kg/m<sup>3</sup>. The idealized shock loading profile at the base of the cantilever was that 20,000 g acceleration during  $0 < t < 160$   $\mu$ s and -20,000 g during  $160 < t < 320$   $\mu$ s, Figure 9.

The model simulated deformation history is illustrated in Figure 10, which shows the same deformation behavior as the experiment. The displacement-time curves of the mass and the bar are plotted in Figure 11(a), and the

relative displacement versus time is plotted in Figure 11(b). To make a direct comparison with the experimental results, the experimental image and the simulation plot at the same time are laid to overlap each other. Figure 12(a) shows the initial un-deformed state at  $t = 0 \mu\text{s}$ , where the cantilever matches perfectly. At  $t = 470 \mu\text{s}$ , which corresponds to the maximum relative displacement, Figure 12(b) shows that simulated  $u_{\text{mass}}$  and  $u_{\text{bar}}$  both are larger than those from experiment.

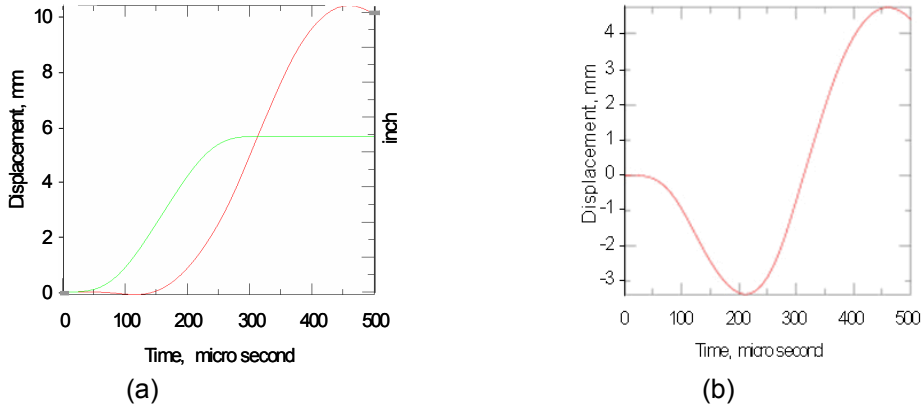


Figure 11 Simulated displacement histories: (a)  $u_{\text{mass}}$  (red) and  $u_{\text{bar}}$  (green), (b)  $u_{\text{rel}} = u_{\text{mass}} - u_{\text{bar}}$ .

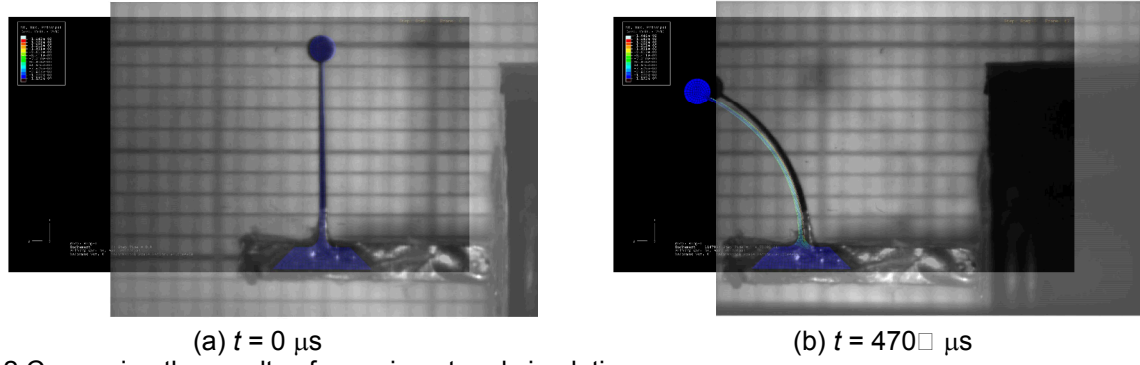
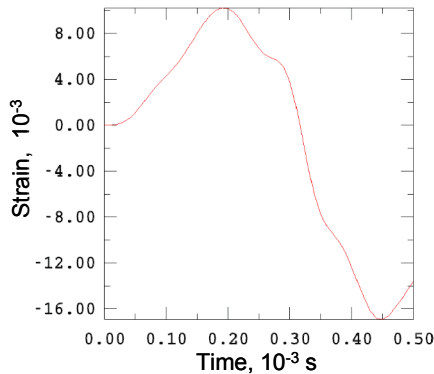


Figure 12 Comparing the results of experiment and simulation.

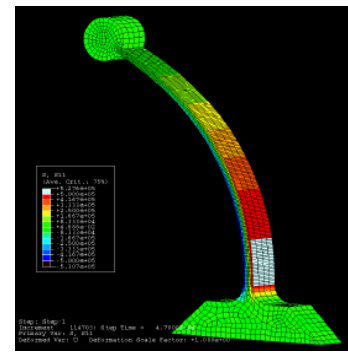
## DISCUSSION

There are several possible reasons that contribute to the minor displacement differences (less than 10%) between the experiment and the simulation of the free end of the bar, including the variations among the actual, measured, and idealized shock profiles, the resolutions of the image and FEM analyses, etc. For the displacement of the mass, the discrepancy between the experiment and the simulation is about 4% larger than that of the free end. The additional factors that affect  $u_{\text{mass}}$  are: (1) the uncertainties of the material properties used, and (2) the actual deformation may be not perfectly 2-D but includes some out-of-plane modes, i.e., out-of-plane bending or torsion. The out-of-plane deformation modes can not be detected from the 2-D image analysis.

The simulated results show that the maximum strain generated is about 0.016. It occurred at  $t_{\varepsilon_{\text{max}}} \approx 470 \mu\text{s}$  and the location was near the base of the cantilever. The maximum compressive and tensile strain was on the left and right side of the cantilever, respectively. The strain history at the location the maximum compressive strain is plotted in Figure 14(a). When the strain rate was at the maximum  $\dot{\varepsilon} \approx 200 \text{ s}^{-1}$ , the corresponding strain was zero. It occurred when the cantilever was sweeping through the un-deformed position. During most of the deformation recorded, the strain rate was on the order of  $10^2 \text{ s}^{-1}$ . Only within a very short period of time, approximately  $t_{\varepsilon_{\text{max}}} - 5 < t < t_{\varepsilon_{\text{max}}} + 5$ , the strain rate was less than  $10 \text{ s}^{-1}$ . At the maximum strain, the corresponding strain rate was zero. Figure 14(b) shows the strain distribution on the tensile side of the beam at  $t = 470 \mu\text{s}$ .



(a)



(b)

Figure 14 (a) Strain history of the region having the maximum compressive strain, located on the left side of the cantilever. (b) Tensile strain distribution on the right side of the cantilever at  $t = 470 \mu\text{s}$ .

The maximum tensile strain 0.016 corresponds to a stress value of 3.8 GPa for the linear elastic material, which is much higher than the measured tensile strength of the LIGA Ni under the quasi-static loading condition,  $\sigma_{ut} = 1.8$  GPa. The simulation used a relatively high value of elastic modulus, assumed no plastic deformation, but gave a larger deformation than experiment. If the model considers elastic-plastic material, the cantilever would have even larger deformation than the elastic material. The comparison between the experiment and simulation suggests there is a significant rate enhancement on the mechanical properties of the material. Furthermore, the rate effect appears to be based on the strain rate history or the averaged strain rate. The instantaneous strain rate along does not explain the behaviors of the structure.

## SUMMARY

The LIGA-fabricated tapered cantilever-mass structure was subjected to 20k g shock loading utilizing Hopkinson bar apparatus. The deformation of the structure was recorded at  $\sim 50,000$  fps for the first 550  $\mu\text{s}$ . No apparent plastic deformation or damage was observed. An elastic model, considering linear material behavior and nonlinear deformation, was used to model the experiment. The simulated deformation matches the experiment well, which indicates significant strain rate effect on material properties. More investigation is needed to understand the high rate behaviors of the microsystem materials and structures.

## ACKNOWLEDGEMENT

The authors thank S.H. Goods for providing LIGA specimens for this investigation.

Sandia is a multiprogram laboratory operated by Sandia Corporation, a Lockheed Martin Company, for the United States Department of Energy under contract DE-AC04-94-AL85000.

## REFERENCES

- [1] J.J. Kelly and S.H. Goods, "LIGA-Based Microsystem Manufacturing: The Electrochemistry of Through-Mold Deposition and Material Properties," SAND2005-2537, Sandia National Laboratories
- [2] *The Properties of Electrodeposited Metals and Alloys*, W.H. Safranek, ed., American Electroplaters and Surface Finishers Society, 1986.